Check for updates

Distribution of rapid pyrolysis products for Hami lignite and its light residue

Wen-Long Mo, [ab] Pei Liu,[b] Yan-Xiong Wang,[b] Gui-Han Zhao,[b] Ya-Ya Ma,*[b] Xing Fan, [b] Xian-Yong Wei [bc] and Akram Naeem [d]

Naomaohu lignite (NL) from Hami, Xinjiang, was ultrasonically extracted with a mixed solvent of CS_2 and acetone (in equal volumes) to obtain the extract residue (ER). The ER was then separated based on density differences with CCl_4 to yield the corresponding light residue (NL-L). The composition and structural characteristics of the light residue were characterized by proximate, ultimate, infrared, and thermogravimetric analyses (TG-DTG). The difference in the distribution of pyrolysis products between NL and NL-L was studied with rapid pyrolysis equipment (Py-GC/MS). The results showed that solvent extraction and density difference can reduce moisture and increase volatile matter. The relative content of oxygen-containing functional groups and aromatic functional groups in NL-L is greater than that in NL. The weight loss profiles of the two samples are the same, and both reach their maximum rate of weight loss at about 440 °C. It can be inferred that the process of ultrasonic extraction and density difference has little impact on the macromolecular structure of the coal. Results from rapid pyrolysis showed that the organic compounds detected in the pyrolysis products of the two samples at 440 °C were mainly aliphatic hydrocarbons and oxygen-containing compounds. The relative content of aliphatic hydrocarbons from NL-L was 11.64%, lower than that of NL, while the content of oxygen-containing compounds was increased by 17.52%.

1. Introduction

The conventional use of coal typically requires high temperatures and pressures, which come with several disadvantages, including the need for expensive equipment, low conversion efficiency, limited added value, and the generation of significant pollutants.[1] The current use of low-rank coal, characterized by high pollution, low efficiency and limited added value should be improved to achieve clean, efficient, and high-value added utilization. Lignite is an important coal resource in China, but its utilization is not high enough due to its high moisture and ash content. Applying the method of solvent extraction to lignite is expected to improve its resource utilization.[2–7]

Due to the complex interactions within the coal's structure, most organic compounds in coal are poorly soluble in common organic solvents. Under appropriate conditions, the extractant penetrates into the network structure of coal, destroying the intermolecular forces, to separate out the soluble organic matter in coal. The selection of different extractants will result in differences between the extracted products and residues.[8] An acetone/CS_2 mixed solvent can effectively extract some organics in coal and swell its macromolecular network structure.[9,10] Another influence on extraction is the treatment method. Yu *et al.*[11] found that ultrasonic/microwave-assisted extraction can effectively improve the efficiency of the extraction of the soluble organic matter in coal.[12] In addition, CCl_4 is used for density difference layering of the residue obtained from extraction, which can remove heavy minerals that cannot be removed by extraction to obtain a light residue.[13]

Zou *et al.*[14] used tetrahydrofuran (THF) to extract two low-rank coals. It was found that, compared with raw coal, the gas yield of the extract residue was higher during pyrolysis in N_2 atmosphere, while the yield of coke was similar. In addition, the relative content of phenols and mononuclear aromatics from the residue is higher than that from raw coal, which might be due to the increased activity of the O atoms in coal by extraction, so that some of the O atoms could be converted into OH during pyrolysis. Zhu *et al.*[15] used the methods of pyridine extraction and steam swelling to treat Naomaohu lignite and Hutubi soft coal and studied the structure and pyrolysis behavior of the corresponding residue. The results showed that the gas yield of the residue by pyrolysis is higher than that from raw coal, while

[a]*College of Chemical and Textile Engineering, Xinjiang University of Science & Technology, Korla 841000, Xinjiang, China*

[b]*State Key Laboratory of Chemistry and Utilization of Carbon Based Energy Resources, Key Laboratory of Coal Clean Conversion & Chemical Engineering Process (Xinjiang Uyghur Autonomous Region), School of Chemical Engineering and Technology, Xinjiang University, Urumqi 830017, Xinjiang, China. E-mail: mayaya1103@126.com*

[c]*Key Laboratory of Coal Processing and Efficient Utilization, Ministry of Education, China University of Mining & Technology, Xuzhou 221116, Jiangsu, China*

[d]*School of Chemical Engineering, Minhaj University Lahore, Lahore 54000, Punjab, Pakistan*

the tar yield from the residue is significantly reduced. The extraction and swelling process also improved the porosity of the coal. Tian *et al.*[16] used a combined method of thermal reflux extraction (with cyclohexanone (CYC) as solvent) and ultrasonic-assisted extraction (with an NMP/CS_2 mixture as solvent) to extract four demineralized coals with different ranks. The results showed that relative contents of organic functional groups, such as C–C, C=O, and fatty hydrogen, in the four residues decreased after removing soluble components. Notably, existing studies focus primarily on the structure and pyrolysis performance of the residues, with limited attention to the specific distribution of pyrolysis products.

In this paper, Naomaohu lignite from Hami, Xinjiang, was extracted under mild conditions with a CS_2/acetone mixture as the solvent to remove soluble organic matter. The residue was then subjected to a density difference stratification treatment with CCl_4 to remove the heavy components in the coal, yielding a light residue. Unlike previous studies, focusing primarily on residue structure and general pyrolysis behavior, this work uniquely provides a quantitative analysis of the distribution of rapid pyrolysis products for both raw coal and its light residue. Infrared spectroscopy and thermogravimetry were used to study the difference in composition and structure between the residue and raw coal. Quantitative analysis of their rapid pyrolysis products was carried out with the help of rapid pyrolysis gas chromatography-mass spectrometry.

2. Experimental

2.1. Raw materials

The raw coal used in this experiment was obtained from Naomaohu coalfield in Hami, Xinjiang, China. Before the experiments, the coal sample was pulverized to a particle size of less than 200 mesh and dried naturally at room temperature for 24 h; the obtained sample was recorded as NL. Solvents used in the experiment included acetone, carbon disulfide, and carbon tetrachloride, all of which were analytically pure reagents produced by Tianjin Yongsheng Fine Chemical Co., Ltd and were refined with a rotary evaporator before use.

2.2. Preparation of light residue

15 g of the coal sample and 150 mL of the equal-volume mixed solvent of acetone and carbon disulfide were placed in a 500 mL beaker at room temperature and subjected to ultrasonic treatment for 30 min. The mixture in the beaker was filtered to obtain the extract liquid and the corresponding residue, and the residue was extracted 20 times until the collected extract liquid was nearly colorless. The residue was then treated with 150 mL of CCl_4 under ultrasonic conditions for 30 min. The resulting mixture was transferred to a 250 mL separating funnel and allowed to stand for 1 h, during which lamination was observed, as shown in Fig. 1. The upper solid phase (containing a certain amount of carbon tetrachloride) was extracted and washed with CS_2, and the light residue was obtained and recorded as NL-L.

2.3. Analysis methods

2.3.1. Proximate analysis. Moisture, ash, and volatile matter from the coal and its light residue were tested according to GB/T212-91, and the fixed carbon content of the two samples was calculated accordingly.

2.3.2. Ultimate analysis. A Vairo ELcube element analyzer was used to measure the relative content of C, H, N, and S elements in the two samples, and the content of the O element was calculated from the difference.

2.3.3. FTIR characterization. The functional groups of the two samples were detected with a Fourier infrared spectrometer (VERTEX 70 RAMI). First, one of the samples was dried under vacuum for 10 h; then, it was fully mixed with KBr powder in a mass ratio of 1 : 160, and the mixture was compressed. The scanning resolution was set as 0.4 cm^{-1}, and the wavelength range was set as 400–4000 cm^{-1} with a wavenumber accuracy of 0.01 cm^{-1}.

2.3.4. Thermogravimetric analysis. The thermogravimetric behavior of each sample was analyzed by heating it from room temperature to 1000 °C at a rate of 10 °C min^{-1} under a nitrogen atmosphere using a thermogravimetric analyzer (SDTQ-600).

2.3.5. Py-GC/MS analysis. From pyrolysis chromatography-mass spectrometry technology, it can be concluded that the sample is instantly pyrolyzed at high temperature under an inert atmosphere, and the chemical bonds of the sample are broken, resulting in the formation of low-molecular-weight volatile compounds. These cracked gas components are separated by gas chromatography and subsequently analyzed by a mass spectrometer to obtain their chromatograms. Qualitative and quantitative analyses of the components can be carried out with the mass spectra of each fragment peak on the
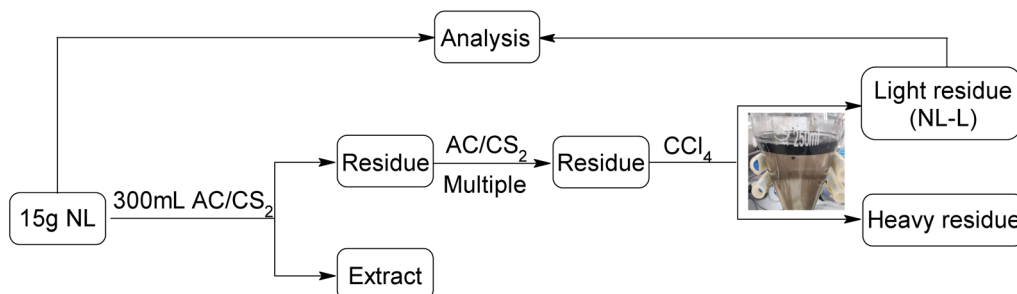

Fig. 1 Preparation process of NL-L.

chromatograms. In this paper, Naomaohu coal and its light residue were tested by Py-GC/MS at 440 °C.

3. Results and discussion

3.1. Proximate and ultimate analyses

It can be seen from Table 1 that Naomaohu lignite presents a higher moisture and ash content, with 39.81% volatile matter. Compared with NL, the ash content of NL-L had decreased by 44.57%, indicating that some minerals in the coal had been removed during the extraction process. While the volatile matter of NL-L was 16.45% higher than that of NL, which might be because the intermolecular force in the coal might be destroyed, and some less volatile components could also be released.[17] Additionally, the rapid decrease in moisture might be derived from the extraction and density difference separation processes with AC/CS$_2$ and CCl$_4$, in which the molecules of H$_2$O were dissolved by the solvents used.

It can also be seen from Table 1 that, compared with NL, the content of C in NL-L increases. This part of C mainly comes from volatile matter and fixed carbon, which is consistent with the increase in fixed carbon and volatile matter in the proximate analysis. The O content and O/C ratio in NL-L are lower than those in NL, indicating that some compounds with oxygen-containing functional groups might be extracted during solvent extraction. The H/C atomic ratio of NL-L decreases, indicating that the mixed extractant of carbon disulfide and acetone shows a significant dissolution effect on compounds

with a high H/C ratio, such as aliphatic and aromatic compounds in coal.[18]

3.2. FTIR analysis

Fourier transform infrared spectroscopy (FTIR) was employed to characterize NL and its light residue (NL-L), and the results are shown in Fig. 2. According to the functional groups of the two samples, four types can be observed: hydroxyl, aliphatic, oxygen-containing, and aromatic-ring groups.

Peaks in the range of 3600–3000 cm^{-1} correspond to the stretching vibration of the hydroxyl hydrogen bond, and the peak shape is wider because several hydroxyl hydrogen bonds can be found in the coal. For NL-L, the intensity of the C=O absorption peak at 1700 cm^{-1} had increased slightly, indicating that some compounds with oxygen-containing functional groups in NL-L might be exposed after solvent extraction. Absorption peaks at 1300–900 cm^{-1} are assigned to the stretching vibration of single bonds, such as C–C, C–O and C–N, and the deformation vibration of hydrogen-containing groups, such as C–H and O–H.

From Fig. 2, the FTIR profile of NL-L is not significantly different from that of NL in the characteristic absorption peak range (900–700 cm^{-1}) of aromatic functional groups. It can also be seen that the trends in the FTIR spectra of NL and NL-L are similar, and only a slight difference in the intensity of each absorption peak can be found, indicating that the ultrasonic extraction process under room temperature did not cause obvious damage to the macromolecular structure of the coal.[19]

Table 1 Proximate and ultimate analyses of the coal samples

Sample	Proximate analysis (wt%)				Ultimate analysis (wt%)					Mol ratio	
	M_{ad}	A_{ad}	V_{ad}	FC_{ad}	C	H	N	S	O^a	H/C	O/C
NL	12.69	8.66	39.81	38.84	61.75	4.91	1.16	0.31	>31.87	0.95	0.39
NL-L	5.07	4.80	46.36	43.77	63.94	4.87	1.21	0.37	>29.61	0.91	0.35

^{a} ad: air dry basis; a: by difference.

Fig. 2 FTIR spectra of NL and NL-L.

Paper

RSC Advances

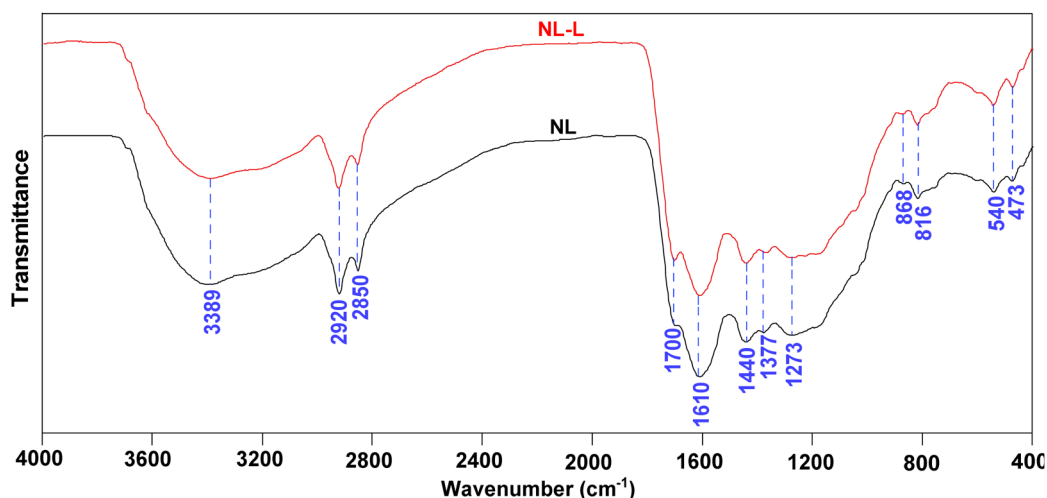### 3.3. FTIR semi-quantitative analysis

According to Fig. 2, the infrared absorption spectra of the two samples can be divided into four regions to discuss the change in the relative content of each functional group. Peak fitting was performed for each absorption peak of the two samples, and the results are shown in Fig. 3. The corresponding functional group attribution and proportion of peak area are shown in Table 2.
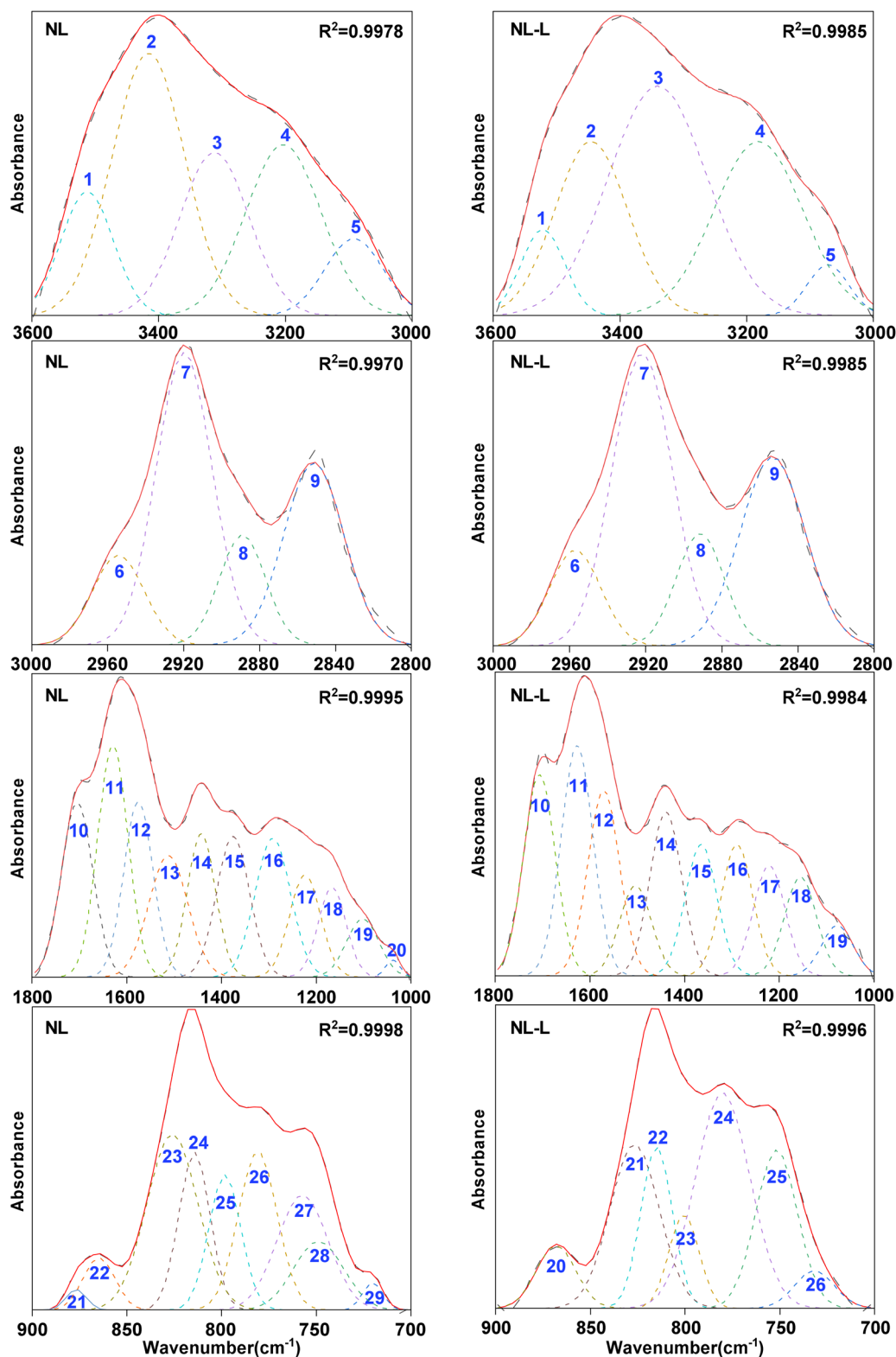

Fig. 3 FTIR peak-fitting profiles of NL and NL-L.

Table 2 Relative content of each functional group in NL and NL-L

Number	Band range per cm	Functional group	Area percentage (%)		Increasing rate (%)
			NL	NL-L	
1	3600–3500	OH–π	11.98	6.66	−44.41
2	3500–3350	Self-associated OH	35.23	22.36	−36.53
3	3350–3260	OH–ether	20.77	39.92	92.20
4	3260–3170	Cyclic–OH	23.72	27.29	15.05
5	3170–3000	OH–N	8.30	3.76	−54.70
6	2950–2930	Aliphatic–CH_3	12.52	12.28	−1.92
7	2930–2900	Asymmetric aliphatic–CH_2	44.11	43.61	−1.13
8	2900–2870	Aliphatic–CH	13.68	13.46	−1.61
9	2870–2850	Symmetric aliphatic–CH_2	29.69	30.64	3.20
10	1800–1700	Carboxylic C=O	12.57	14.43	14.80
11	1700–1600	Conjugated C=O	16.01	16.52	3.19
12	1570–1480	Aromatic C=C	22.54	19.77	−12.29
13	1480–1400	Asymmetric CH_3^-, CH_2^-	9.24	11.76	27.27
14	1400–1240	Symmetric deformation–CH_3	21.84	18.87	−13.60
15	1240–1160	C–O phenols	12.91	15.04	16.50
16	1160–1090	Grease C–O	4.32	3.61	−16.44
17	1090–1030	Alkyl ethers	0.57	—	—
18	900–860	Five adjacent H deformation	5.74	6.42	11.85
19	860–810	Four adjacent H deformations	38.25	34.30	−10.33
20	810–750	Three adjacent H deformations	45.06	55.38	22.90
21	750–720	Two adjacent H deformations	10.95	3.89	−64.47

In the range of 3600–3000 cm^{-1}, after the ultrasonic extraction–delamination treatment of NL, the relative content of OH–π, self-associated OH and OH–N hydrogen bonds decreased significantly by 44.41%, 36.53%, and 54.70%, respectively. The relative content of cyclic –OH hydrogen bonds increased by 15.05%, while the relative content of OH–ether hydrogen bonds increased significantly, with an increase of 92.20%. At the vibration absorption peak of aliphatic functional groups at around 3000–2800 cm^{-1}, the relative contents of CH_3, CH_2 and CH in NL-L are slightly lower than those in NL, where CH_2 is dominant.

For the peak of oxygen-containing functional groups at around 1800–1000 cm^{-1}, the relative content of C=O from carboxylic acid in NL-L increased by 14.80%. The relative content of aromatic C=C decreased by 12.29%, which might be due to the strong extraction effect of carbon disulfide on aromatic-ring-containing compounds in NL.[20] In the range of 900–700 cm^{-1} of aromatic-ring peaks, benzene ring trisubstituted groups are dominant in NL and NL-L, and the relative content of benzene ring trisubstituted groups in NL-L is increased by 22.90%.

3.4. TG-DTG analysis

The weight loss behavior of NL and its light residue (NL-L) was tested by the thermogravimetry method under the condition of pure nitrogen. The weight loss profile (TG) and weight loss rate curve (DTG) of each sample are shown in Fig. 4.

Both TG profiles show that the trends in weight loss of NL and NL-L are essentially similar. Up to 260 °C, the drying and degassing stages occur. At this point, the weight loss rate of NL
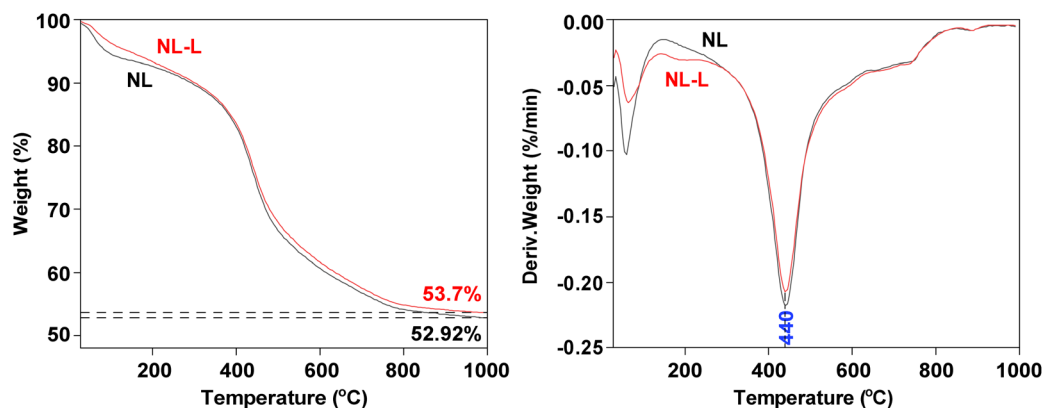

Fig. 4 TG and DTG curves of NL and NL-L.

is higher than that of NL-L, which might result from NL containing more water (12.69%). The temperature range of 320–650 °C is assigned to the main thermal decomposition stage. In this region, there is an obvious weight loss rate peak for each sample, due to the cracking of its macromolecular skeleton. Additionally, the final weight losses of NL and NL-L are 47.08% and 46.30%, respectively, indicating that there is little difference in weight loss between the two samples.
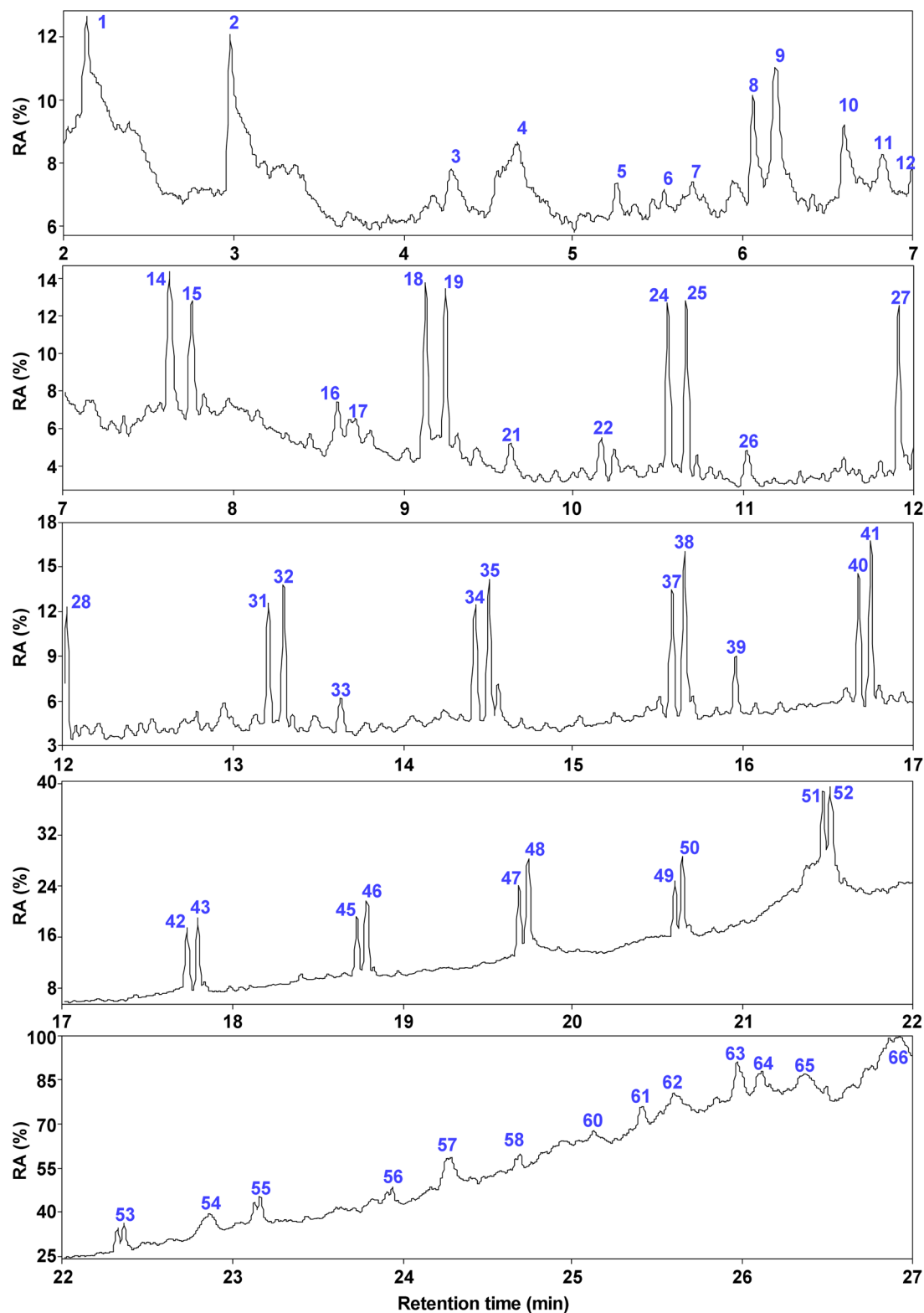

Fig. 5 Total ion chromatogram of NL.

It can be seen from the DTG profile that up to 200 °C, NL and NL-L show the first weight loss rate peak at 60 °C, because the free water in the coal is vaporized by heating, and the gas adsorbed in the coal pores is also discharged.[21] As the temperature exceeds 200 °C, a decarboxylation reaction occurs, and CO_2 may be present in the product gas. In other words, the drying and degassing processes were nearly complete between room temperature to 260 °C. When the temperature rises to
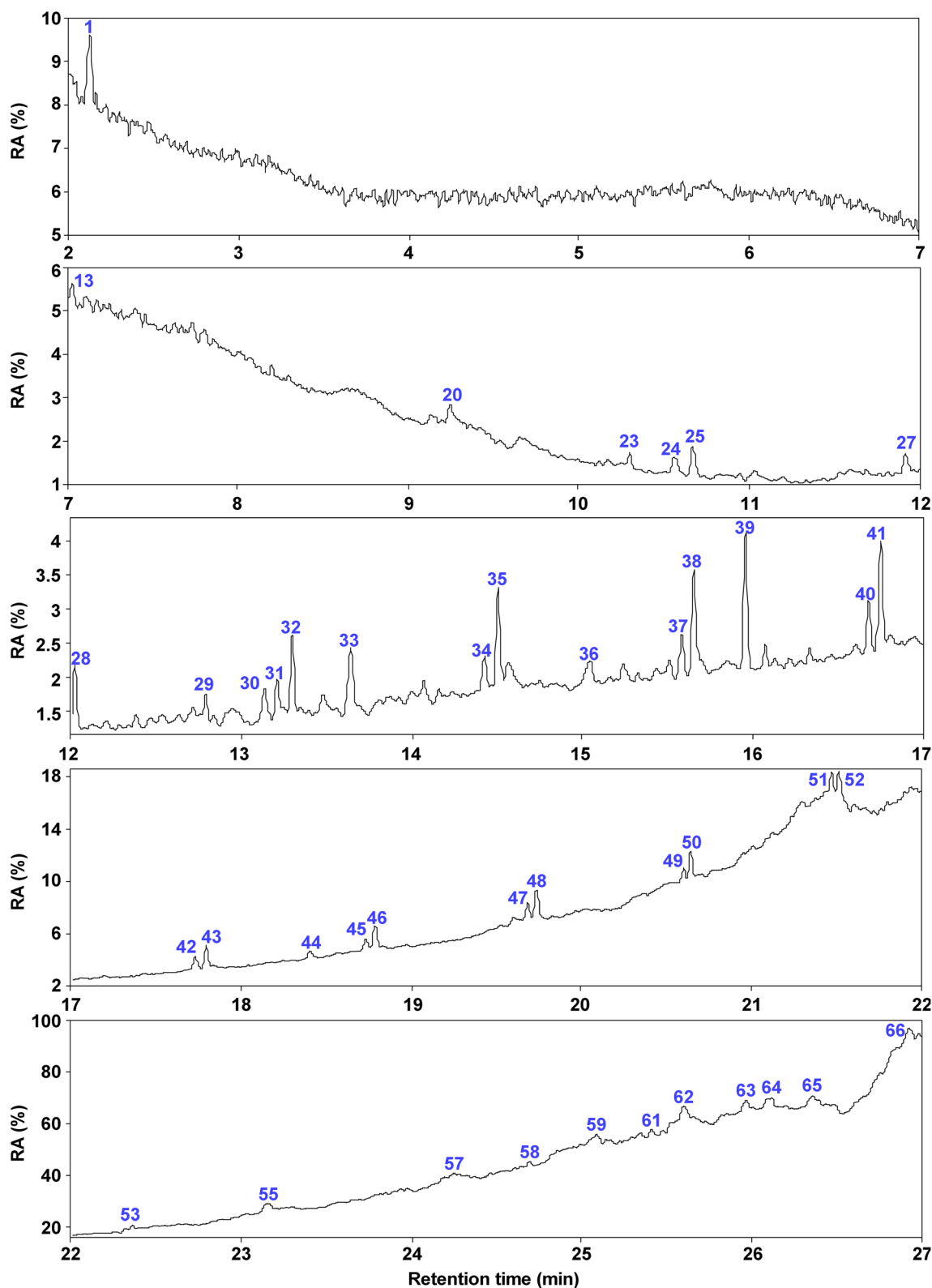

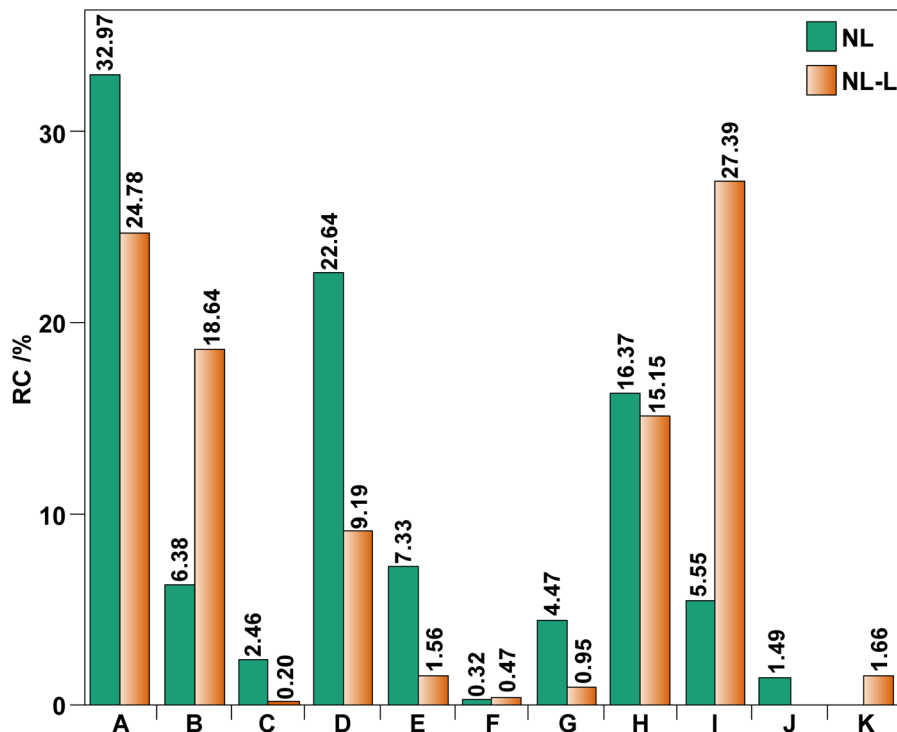Fig. 6 Total ion chromatogram of NL-L.

Fig. 7 Relative content of group components from NL and NL-L (A: *N*-alkanes; B: branched alkanes; C: cyclanes; D: olefins; E: arenes; F: acids; G: alcohols; H: esters; I: phenols; J: N-containing compounds; K: others).

440 °C, the weight loss rates of both coal samples reach their maximum, indicating that this temperature range represents the most violent stage during coal pyrolysis, during which a large amount of volatile matter escapes, and coal tar and pyrolysis gas are simultaneously produced.[22–24] Above 600 °C, condensation reactions may occur, leading to the reformation of the aromatic-ring structure. Semicoke begins to form, and tar precipitation decreases, and a small amount of condensed small molecules might be generated.

3.5. Py-GC/MS analysis

Fig. S1 shows the original total ion flow chromatograms of the rapid pyrolysis products of NL and NL-L at 440 °C. A retention time of 2–27 min is selected for analysis. The results are shown in Fig. 5 (NL) and 6 (NL-L). The detected compounds are classified into 11 groups, and the results are shown in Tables S1–S11 and Fig. 7. There are 57 compounds that can be detected in NL pyrolysis products, mainly including alkanes, olefins, aromatics, alcohols, and esters, and the content of alkanes and olefins is as high as 64.45%. Among them, there are 21 kinds of alkanes, most of which are normal alkanes, as well as 15 kinds of olefins, eight kinds of aromatic hydrocarbons, four kinds of alcohols and five kinds of esters (Tables S1–S11). A total of 45 compounds can be detected in NL-L pyrolysis products, and the relative content of alkanes and olefins is as high as 52.81%, and the rest of the compounds are mostly esters and phenols.[25–27]

It can be seen from Fig. 7 that, after solvent extraction–delamination treatment, the relative content of normal alkanes from NL-L decreases, while the content of branched alkanes

increases significantly, indicating that the treatment method can improve the added value of coal pyrolysis products in terms of alkane compounds.[28] The olefin content from NL-L decreases significantly from 22.64% to 9.19%, which might be due to the high solubility of olefin compounds in an acetone/carbon disulfide mixed solvent.[29] It can also be seen from Fig. 7 that the content of alcohols from NL-L decreases from 4.47% to 0.95%. It is speculated that acetone has high solubility for alcohols.[10]

Compared to NL, the content of arenes from NL-L decreases from 7.33% to 1.56%, and the content of phenols increases sharply from 5.55% to 27.39%. The reason might be that the method of ultrasonic extraction could improve the activity of oxygen atoms in the coal. During the rapid pyrolysis process, some oxygen atoms were converted to OH, which could attack the benzene ring to form phenolic compounds.[14,30] Meanwhile, after solvent extraction, the oxygen-containing compounds in the pyrolysis products of NL-L were increased, consistent with the FTIR results showing an increase in oxygen-containing functional groups.[31,32]

4. Conclusions

In this work, Naomaohu lignite was extracted to obtain its light residue. The TG profiles of Naomaohu lignite and its light residue are essentially the same, and both reach the maximum rate of weight loss at about 440 °C. At this temperature, the distributions of rapid pyrolysis products of the two samples show that the products are composed mainly of aliphatic hydrocarbons and oxygenates, and the relative content of

alkanes and olefins is dominant in the aliphatic hydrocarbons. After solvent extraction–delamination treatment, the relative content of aliphatic hydrocarbons from NL-L by pyrolysis decreases, in which *n*-alkanes and olefins decrease significantly. In addition, the content of oxygenates increases to a certain extent, and the increase in phenolic compounds is more obvious, which might be related to the increase in activity of O atoms in the light residue caused by the extraction process.

Conflicts of interest

There are no conflicts to declare.

Data availability

The data supporting this article have been included as part of the SI. Original total ion chromatograms of NL and NL-L in Fig. S1. *N*-alkanes detected in NL and NL-L in Table S1. Branched alkanes detected in NL and NL-L in Table S2. Cyclanes detected in NL and NL-L in Table S3. Alkenes detected in NL and NL-L in Table S4. Arenes detected in NL and NL-L in Table S5. Acids detected in NL and NL-L in Table S6. Alcohols detected in NL and NL-L in Table S7. Esters detected in NL and NL-L in Table S8. Phenols detected in NL and NL-L in Table S9. Nitrogen-containing organic compounds detected in NL and NL-L in Table S10. Other organic compounds detected in NL and NL-L in Table S11. See DOI: **https://doi.org/10.1039/d5ra03915k**.

Acknowledgements

References

1 B. J. Fu, Y. X. Liu, Y. Li, *et al.*, The research priorities of Resources and Environmental Sciences, *Geogr. Sustain.*, 2021, **2**(2), 87–94.

2 X. Li, C. W. Li, H. J. Zhang and W. F. Li, Analysis on the status and problems of lignite application in China, *Appl. Chem. Ind.*, 2020, **49**(5), 1226–1230.

3 H. Kan, Y. Wang, W. L. Mo, X. Y. Wei, H. Y. Mi, K. J. Ma, M. X. Zhu, W. C. Guo, J. Guo, J. M. Niu and X. Fan, Effect of solvent swelling with different enhancement method on the microstructure and pyrolysis performance of Hefeng subbituminous coal, *Fuel*, 2023, **332**, 126066.

4 G. H. Liu, Z. M. Zong, X. Y. Wei, F. Y. Ma, W. L. Mo, *et al.*, Observing the structural variation of Dahuangshan lignite and four derived residues by non-destructive techniques and flash pyrolysis, *Fuel*, 2019, **269**, 117335.

5 X. B. Hu, H. Xu, W. L. Mo, X. Fan, W. C. Guo, J. Guo, J. M. Niu, H. Y. Mi, Y. Y. Ma and X. Y. Wei, Effect of sequential thermal dissolution on the structure and

6 Z. K. Li, X. Y. Wei, H. L. Yan, Z. M. Zong, *et al.*, Advances in Lignite Extraction and Conversion under Mild Conditions, *Energy Fuels*, 2015, **29**(11), 6869–6886.

7 M. Ding, Y. P. Zhao, X. Y. Wei, X. Fan, Z. M. Zong, *et al.*, Sequential extraction and thermal dissolution of Shengli lignite, *Fuel Process. Technol.*, 2015, **135**, 20–24.

8 Y. Y. Ma, F. Y. Ma, W. L. Mo and Q. Wang, Five-stage sequential extraction of Hefeng coal and direct liquefaction performance of the extraction residue, *Fuel*, 2020, **266**, 117039–117048.

9 Y. P. Zhao, J. Xiao, M. Ding, E. G. Eddings, X. Y. Wei, X. Fan, *et al.*, Sequential extraction and thermal dissolution of Baiyinhua lignite in isometric CS2/acetone and toluene/methanol binary solvents, *Energy Fuels*, 2016, **30**(1), 47–53.

10 X. Guo, S. J. Li, Y. Z. Chai, J. Wei, C. B. Xu and F. Guo, Molecular characteristics of organic matter obtained from biochar by carbon disulfide/acetone synergistic extraction, *Environ. Chem.*, 2022, **19**(2), 82–89.

11 X. Y. Yu, X. Y. Wei, Z. K. Li, Y. Chen, Z. M. Zong, F. Y. Ma and J. M. Liu, Comparison of three methods for extracting Liuhuanggou bituminous coal, *Fuel*, 2017, **210**, 290–297.

12 C. Jv, *et al.*, Analysis of Carbon Tetrachloride-Extractable Species from Daxing Bituminous Coal, *Appl. Sci.*, 2020, **10**(2), 494.

13 Z. F. Wu, X. Y. Wei, W. L. Mo, X. Fan, *et al.*, Catalytic hydroconversion of the light residue from Yinggemajianfeng lignite over a solid superacid, *Fuel*, 2021, 122470.

14 L. Zou, L. J. Jin, Y. Li, S. W. Zhu and H. Q. Hu, Effect of tetrahydrofuran extraction on lignite pyrolysis under nitrogen, *J. Anal. Appl. Pyrolysis*, 2015, **112**, 113–120.

15 P. Zhu, A. Luo, F. Zhang, *et al.*, Effects of extractable compounds on the structure and pyrolysis behaviours of two Xinjiang coal, *J. Anal. Appl. Pyrolysis*, 2018, **133**, 128–135.

16 B. Tian, Y. Y. Qiao, Y. Y. Tian, K. C. Xie, Q. Liu and H. F. Zhou, FTIR study on structural changes of different–rank coals caused by single/multiple extraction with cyclohexanone and NMP/CS$_2$ mixed solvent, *Fuel Process. Technol.*, 2016, **154**, 210–218.

17 F. J. Liu, X. Y. Wei, *et al.*, Investigation on structural features of Shengli lignite through oxidation under mild conditions conditions, *Fuel*, 2013, **109**, 316–324.

18 Z. Qin, P. Chang, L. Ma, *et al.*, Preparation and modulation of a novel thin-walled carbon foam, *Int. J. Min. Sci. Technol.*, 2019, **29**(2), 281–287.

19 Z. Y. Niu, G. J. Liu, H. Yin, C. C. Zhou, *et al.*, Effect of pyridine extraction on the pyrolysis of a perhydrous coal based on in-situ FTIR analysis, *J. Energy Inst.*, 2019, **92**(3), 428–437.

20 D. L. Shi, X. Y. Wei, B. Chen, X. Fan, *et al.*, The Enrichment of Condensed Arenes in Geting Bituminous Coal, *Energy Sources, Part A Recovery, Util. Environ. Eff.*, 2013, **35**(20), 1898–1904.

21 X. K. Shan, S. L. Zhao, Y. Y. Ma, W. L. Mo, X. Y. Wei, *et al.*, Analysis of Pyrolysis Performance and Molecular Structure

of Five Kinds of Low-Rank Coals in Xinjiang Based on the TG-DTG Method, *ACS Omega*, 2022, **7**(10), 8547–8557.

22 W. L. Mo, X. K. Shan, X. Q. He, X. Y. Wei, X. Fan, *et al.*, Functional Group Characteristics and Pyrolysis/Combustion Performance of Karamay OS Based on FT-IR and TG-DTG Analyses, *ACS Omega*, 2021, **6**(42), 27684–27696.

23 W. L. Mo, Z. F. Wu, X. Q. He, X. Y. Wei, X. Fan, F. Y. Ma, *et al.*, Functional group characteristics and pyrolysis/combustion performance of fly ashes from Karamay oily sludge based on FT-IR and TG-DTG analyses, *Fuel*, 2021, **296**, 120669.

24 Y. Wang, Y. Y. Ma, W. L. Mo, W. T. Gong, F. Y. Ma, X. Y. Wei, X. Fan and S. P. Zhang, Functional groups of sequential extracts and corresponding residues from Hefeng sub-bituminous coal based on FT-IR analysis, *J. Fuel Chem. Technol.*, 2021, **49**(07), 890–901.

25 J. Li, Y. Qiao, P. Zong, *et al.*, Fast pyrolysis characteristics of two typical coastal zone biomass fuels by thermal gravimetric analyzer and down tube reactor, *Bioresour. Technol.*, 2019, **283**, 96–105.

26 X. Fan, X. Y. Wei and Z. M. Zong, Application of gas chromatography/mass spectrometry in studies on separation and identification of organic species in coals, *Fuel*, 2013, **109**, 28–32.

27 X. Y. Cheng, M. Li, C. G. Sun, Q. Jin, J. J. Li and R. S. Xu, GC/MS Analysis of Bituminous and Lignite Extracts by Different Solvents, *Coal Convers.*, 2020, **43**(02), 1–10.

28 Y. N. Wang, X. Y. Wei, Z. K. Li, *et al.*, Extraction and thermal dissolution of Piliqing subbituminous coal, *Fuel*, 2017, **200**, 282–289.

29 D. K. Sharma, H. Dhawan, T. Morgan and M. Crocker, Py-GCMS studies of Indian coals and their solvent extracted products, *Fuel*, 2019, **256**, 115981.

30 Y. Liu, L. J. Yan, P. Lv, L. Ren, *et al.*, Effect of n-hexane extraction on the formation of light aromatics from coal pyrolysis and catalytic upgrading, *J. Energy Inst.*, 2020, **93**(3), 1242–1249.

31 S. B. Singh and S. A. Dastgheib, Characteristics of graphene oxide-like materials prepared from different deashed-devolatilized coal chars and comparison with graphite-based graphene oxide, with or without the ultrasonication treatment, *Carbon*, 2024, **228**, 119331.

32 S. B. Singh and M. De, Thermally exfoliated graphene oxide for hydrogen storage, *Mater. Chem. Phys.*, 2020, **239**, 122102.